



## CTAB modified nanoporous carbon for the adsorption of chromate ions from industrial wastewater

Mansoor Anbia\*, Seyyed Ershad Moradi

*Research Laboratory of Nanoporous Materials, Faculty of Chemistry, Iran University of Science and Technology, Narmak, Tehran 16846, Iran*

*Tel. +982177491204; Fax +982177491204; email: anbia@iust.ac.ir*

Received 20 April 2009; accepted 18 March 2010

---

### ABSTRACT

In the present study, cetyltrimethyl ammonium bromide (CTAB) was coated on the surface of ordered mesoporous carbon (OMC) and was used as an adsorbent to remove hexavalent chromium (Cr(VI)) from aqueous solution. The structural order and textural properties of this mesoporous adsorbent was studied by XRD and nitrogen adsorption. The amount of CTAB on the carbon surface was confirmed by TGA analyses. Adsorption experiments were conducted in the batch mode to evaluate the effect of variables of contact time, solution pH, dose of adsorbents (CTAB-OMC and OMC) and temperature, on the amount of adsorption. Maximum adsorption of chromium was observed at solution pH 4. The mechanism of adsorption was found to be the electrostatic attraction of acid chromate ion towards protonated CTAB-OMC. Adsorption equilibrium was achieved within 3–4 h for initial concentrations of Cr(VI) of 10–100 mg/L. Maximum monolayer capacity of CTAB-OMC was observed as 1.4 mmol/g at pH 3 and temperature of 313 K. The adsorption isotherms of chromate ion were in agreement with the Langmuir model.

**Keywords:** Mesoporous; Carbon; Surfactant; Chromate; Adsorption; Langmuir; CTAB

---

### 1. Introduction

The presence of chromate and other chromium anions in various sources of water is an important issue, since the toxicity of these species can result in death, if are taken either over a long period or present in high concentrations. The chemical form of chromium determines its potential toxicity; as Cr(VI) is believed to be more carcinogenic in humans than Cr(III) species [1]. The carcinogenic and toxicity of Cr(VI) are based on its oxidation state where the chromate anion resembles the form of sulfate and phosphate [2]. Hence, the regulation for the limitation of Cr(VI) concentration in water should be highlighted

and emphasized in each and every country. Limits of chromium concentration in water differ in almost every country. As a guideline, World Health Organization (WHO) recommended a maximum level of 0.050 mg/L for Cr(VI) in drinking water [3] and the National Institute for Occupational Safety and Health (NIOSH) proposed that the level of chromium should be reduced to  $10^{-3}$  mg/L [4].

A number of treatment methods for the removal of metal ions from aqueous solutions including ion exchange, electrochemical reduction, evaporation, solvent extraction, reverse osmosis, chemical precipitation, membrane filtration and adsorption have been reported [5]. Most of these methods, however, involve high capital costs and lack of suitability for small-scale industries. On the other hand, the adsorption process is

---

\*Corresponding author

generally known to be one of the most effective techniques for the removal of hazardous metals. As a promising method, the adsorption technique has been studied for the removal of chromate ions.

Adsorbents with strong affinity and high loading capacity have been developed for target cations through the surface modification of various substrates, such as polymers and clays with metal complexing groups [6, 7]. Carbon is the most common adsorbent material, which has a huge specific surface area, plentiful micro and macro pores, and a high adsorption capacity. This adsorbent is economically favorable because it can be made from various low-cost materials of high carbonaceous contents including wood, coal, petroleum coke, sawdust, and coconut shell [8].

Recently, a surface-modification technique has been reported to enhance the adsorption rate and capacity of carbon-based adsorbents [8–9]. Surfactants are adsorbed onto the solid surfaces and change the surface properties of the interfacial areas. In recent years, the application of surfactants in the treatment processes of water and wastewater streams has been increased [10–14].

Recently, Ryoo et al. prepared ordered mesoporous carbons (CMK-*x*) from mesoporous silica templates such as MCM-48, SBA-1 and SBA-15 using sucrose as the carbon source. Mesoporous carbon materials with ordered pore structure, high pore volume, high specific surface area, and tunable pore diameters can be prepared using the hard template method [15]. Due to its open-pore structure and mesoporous properties, mesoporous carbon provides marked advantages over typical activated carbons in the adsorption and diffusion processes [16–20]. Achievements in the development of mesoporous materials have been reported, particularly in the area of adsorbent and catalysis manufacturing. Recently, the adsorption of chromate and other heavy metal ions using mesoporous carbon was reported [21–23].

In this study, the effect of a cationic surfactant, cetyltrimethylammonium bromide (CTAB) on the adsorption of Cr(VI) onto the ordered mesoporous carbon was investigated. The influence of the surfactant was analyzed in terms of both adsorption kinetics and adsorption isotherms for Cr(VI). The effect of pH on the adsorption was also investigated. Furthermore, Langmuir and Freundlich adsorption isotherms were studied to explain the sorption mechanism.

## 2. Materials and methods

### 2.1. Materials

The chemicals used were tetraethyl orthosilicate (TEOS) as a source of silica, CTAB as a surfactant,

sodium hydroxide (NaOH), sodium fluoride (NaF), and deionized water for the synthesis of mesoporous silica (MCM-48), and sucrose as a source of carbon, potassium dichromate ( $K_2Cr_2O_7$ ) and sulfuric acid ( $H_2SO_4$ ) as a catalyst for the synthesis of mesoporous carbon. All chemicals were of analytical grade and were purchased from Merck.

### 2.2. Synthesis of silica template and OMC

High quality MCM-48 material was prepared following the synthesis procedure reported by Shao et al. [24]. Accordingly, 1.25 g sucrose and 0.14 g  $H_2SO_4$  were dissolved in 5.0 g  $H_2O$ . 1 g of MCM-48 was added to this solution. The sucrose solution corresponded approximately to the maximum amount of sucrose and sulfuric acid that could be contained in the pores of 1 g MCM-48. The resultant mixture was dried in an oven at 373 K. The oven temperature was subsequently increased to 433 K. After 6 h at 433 K, the MCM-48 silica containing the partially carbonizing organic masses was added to an aqueous solution consisting of 0.75 g sucrose, 0.08 g  $H_2SO_4$  and 5.0 g  $H_2O$ . The resultant mixture was dried again at 373 K; the oven temperature was subsequently increased to 433 K. This powder sample was heated up to 1173 K under a vacuum condition using a fused quartz reactor equipped with a fritted disk. The obtained carbon-silica composite was washed twice with 1 M NaOH solution of 50% ethanol and 50%  $H_2O$  at 363 K, in order to completely dissolve the silica template. The carbon samples obtained after the silica removal were filtered, washed with ethanol and dried at 393 K.

### 2.3. Chemical modification of OMC

Chemical modification of the prepared ordered-mesoporous carbon was conducted by immersing 5 g of adsorbent in 100 ml of CTAB solution of critical micellar concentration for 4 h. Adsorbents were then separated using Whatman filter paper, rinsed with deionized water, dried in an oven overnight at 383 K, sieved to the required sizes and stored in desiccators for further applications.

### 2.4. Characterization

The X-ray diffraction patterns were recorded on a Philips 1830 diffractometer using  $Cu K\alpha$  radiation. The diffractograms were recorded in the  $2\theta$  range of 0.8–10 with a  $2\theta$  step size of  $0.01^\circ$  and a step time of 1 s. Adsorption-desorption isotherms of the synthesized samples were prepared at 77 K on a micromeritics

model of ASAP 2010 sorptometer to determine the average pore diameter. Pore-size distributions were calculated by the Barrett-Joyner-Halenda (BJH) method, while surface area of the samples was measured by Brunauer-Emmet-Teller (BET) method. Thermal analysis was carried out using a NETZSCH STA449C analyzer. The instrument settings were a heating rate of 10°C/min and a nitrogen atmosphere with a flow rate of 100 mL/min. About 25 mg of a ground adsorbent sample was used for each particular measurement. The differential weight loss was calculated from the weight-loss curve, where peaks represent the weight loss.

### 2.5. Adsorption studies

A stock solution of 200 mg/L of Cr(VI) was prepared by dissolving an appropriate amount of the Cr(VI) in ultra-pure water (18 MΩ cm) derived from a Milli-Q plus 185 water purifier. Batch adsorption experiments were conducted by agitating the Cr(VI) solutions in 500-mL amber Winchester bottles on a Gallenkamp incubator shaker. The shaker was set at either temperature of 293, 303 and 313 K, and a speed of 150 rpm. Initial solution concentrations of 10–100 mg/L were prepared by pipetting out the required amounts of Cr(VI) from the stock solution. The volume of the solution in each bottle was maintained at 500 mL and the solutions were adjusted to pH 5. About 0.01 g of each adsorbent was accurately weighed on the aluminum foils using a Sartorius (Model BP 201D) analytical balance. The adsorbents were transferred into the bottles containing 50 mL of the solutions. The bottles were shaken vigorously for various periods in the incubator shaker (New Brunswick Scientific C25 Model).

The amount of the adsorbed Cr(VI) was calculated by subtracting the amount found in the supernatant liquid from the initial amount of Cr(VI). The concentration of Cr(VI) was measured by means of UV-Vis spectrophotometer (UV mini 1240 from Shimadzu). Absorbance was measured at a wavelength ( $\lambda_{\max}$ ) of 372 nm [25]. Centrifugation was used prior to the analysis in order to avoid the potential interference from suspended scattering particles during the UV-Vis analysis. The adsorption capacities were calculated based on the differences among the concentrations of solutes before and after the adsorption according to the following equation [26]

$$q_e = \frac{(C_0 - C_e)V}{W}, \quad (1)$$

where  $q_e$  is the concentration of the adsorbed solute (mmol/g);  $C_0$  and  $C_e$  are the initial and final (equilibrium) concentrations of the solute in solution

(mmol/L);  $V$  (mL) is the volume of the solution and  $W$  (g) is the mass of the adsorbent.

### 2.6. Adsorption kinetics of Cr(VI)

Equilibrium of Cr(VI) adsorption onto the adsorbents was measured by mixing 60 mg of the adsorbents by 15 mL of distilled water in a 500-mL flask for about 10 min. A volume of 285 mL of Cr(VI) solution was quickly introduced into the flask (keeping the concentration of the resulting solutions at 50 mg/L) and continuously stirred at 293 K. Samples were taken by fast filtration at particular time intervals. The concentration of residual Cr(VI) in the solution was measured and the amount of adsorption ( $q_t$ ) was calculated according to the following equation [27].

$$q_t = \frac{(C_0 - C_t)V}{W}, \quad (2)$$

where  $q_t$  is the amount of adsorption at time  $t$ ,  $C_0$  is the initial concentration of Cr(VI) in the solution,  $C_t$  is the concentration of Cr(VI) at time  $t$ ,  $V$  is the volume of Cr(VI) solution, and  $m$  is the mass of OMC and CTAB-OMC.

## 3. Results and discussions

### 3.1. Characterization of the CTAB-OMC and OMC samples

The prepared mesoporous carbon samples in this study were characterized by Nitrogen adsorption-desorption analysis and X-ray diffraction (XRD) techniques.

Nitrogen physisorption is the method more adequate to investigate the mesoporous materials. This method gives information on the specific surface area and the pore diameter. Calculating the pore diameters of mesoporous materials using the BJH method is very common. Former studies show that the application of the BJH theory gives appropriate qualitative results which allow a direct comparison of relative changes between different mesoporous materials.

The nitrogen sorption isotherms of the OMC and CTAB-OMC, are of type IV shape. Interestingly, the pore size distributions are essentially the same as before acid oxidation. The adsorption uptakes at relative pressures close to  $p/p_0 = 0$  are identical. However, the total uptakes are slightly different, increasing with the surface modification with cationic surfactant (CTAB). As shown in Table 1, the increase in the specific surface areas is 5.6% and the decrease in the pore volumes is 10.1%, respectively. From the nitrogen sorption isotherms (Fig. 1) of mesoporous carbons before

Table 1  
Textural parameters of the OMC and CTAB-OMC employed in this study

Adsorbent	d spacing (nm)	$A_{\text{BET}}$ ( $\text{m}^2 \text{g}^{-1}$ )	$V_{\text{P}}$ ( $\text{cm}^3 \text{g}^{-1}$ )
OMC	3.4	1010.5	0.69
CTAB-OMC	3.0	1067.4	0.62

and after chemical modification, it can be seen that after chemical modification the obtained carbons still have type IV isotherms, indicating that mesoporosity is preserved. The modification leads to an increase in the total uptake of the modified carbons, which reflects the increase of the total pore volume resulting from surfactant modification. The modified mesoporous carbons essentially keep the bimodal pore size distribution, which is characteristic of the parent OMC. The textural parameters which are listed in Table 1, clearly confirm the structural changes of modified OMC.

In order to check the structural degradation, XRD data of CTAB-OMC and OMC were obtained. Figure 2 shows the XRD peaks of the samples. The XRD patterns of CTAB-OMC show three diffraction peaks that can be indexed to (110), (210), and (220) in the  $2\theta$  range from  $0.8^\circ$  to  $10^\circ$ , representing well-ordered cubic pores [28]. The XRD patterns of OMC carbon and CTAB-OMC (Figure 2) show well-resolved reflections indicating that OMC carbon nicely maintains its original structure even after the modification by cationic surfactant. For CTAB-OMC sample, the cubic structure of OMC was well maintained; but, the XRD reflections become less pronounced. That might be either due to the partial damage of the mesoporous (cubic) structure or due to the decreased contrast between the walls and

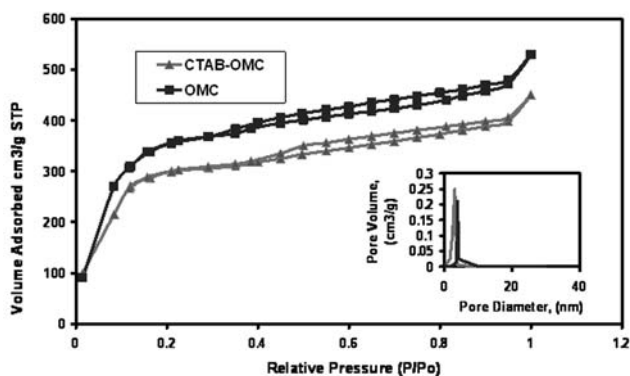


Fig. 1. Adsorption-desorption isotherms of nitrogen at 77 K on OMC and CTAB-OMC. The insert shows the BJH pore size distribution calculated from the desorption branch of the isotherm.

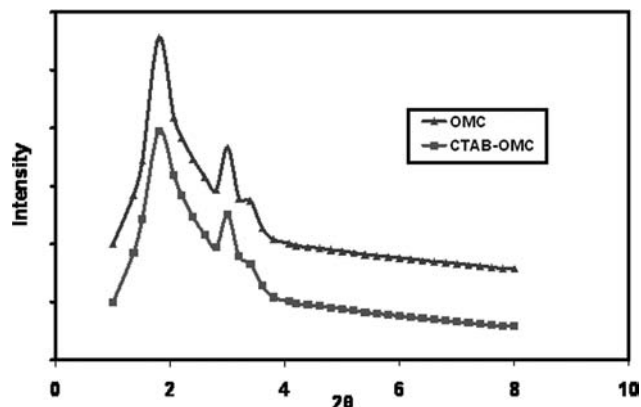


Fig. 2. XRD pattern of CTAB-OMC and OMC.

pores, because of the cleavage of the carbon species from the pore walls.

Figure 3 shows thermogravimetric analysis (TGA) curve of the CTAB-OMC using a nitrogen atmosphere and a heating rate of  $5^\circ\text{C min}^{-1}$ . The weight loss centered at  $220^\circ\text{C}$  is due to the decomposition of CTAB in nitrogen (the melting and decomposition temperatures for CTAB are around  $230^\circ\text{C}$ ). The weight of the sample at  $400^\circ\text{C}$  is about 90.2% of that for the starting CTAB-OMC. It can be concluded that the content of CTAB in OMC is about 10 wt%.

### 3.2. Adsorption studies

#### 3.2.1. Effect of contact time and amount of sorbent

In order to determine the equilibration time for the maximum uptake and the kinetics of the adsorption process, the adsorption of chromate ions onto ordered mesoporous carbon adsorbents were studied. From the results which are shown in Figure 4, it is seen that the rate of uptake for the chromate is rapid

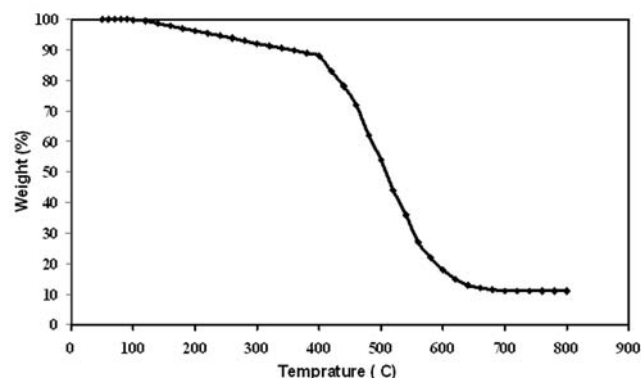


Fig. 3. The TGA plots of the CTAB-OMC.



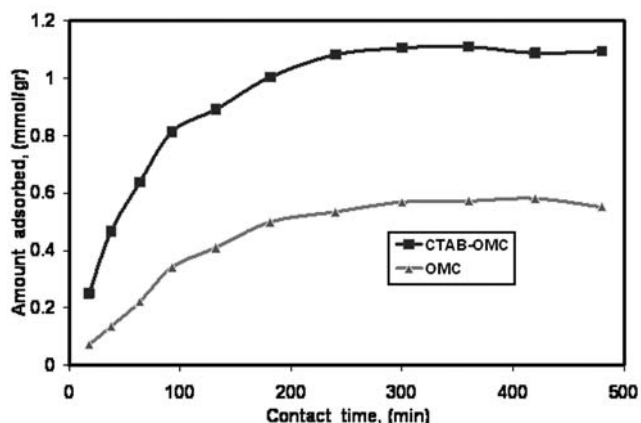


Fig. 4. Effect of contact time on removal of chromate ( $\text{Cr(VI)} = 100 \text{ mg/L}$ , agitation speed = 150 rpm, adsorbent dosage = 0.2 g/L, room temperature =  $298 \pm 1 \text{ K}$ ).

at the beginning and 50% of the adsorption is completed within 60 min. Figure 4 also indicates that the equilibrium time is reached within 220 min. Thus, for all equilibrium adsorption studies, the contact period was kept 360 min. The effect of variation in the amount of carbonaceous adsorbents on the chromium removal is shown in Figure 5. The amount of CTAB-OMC and OMC were varied from 0.05 to 0.5 g/L at an initial chromium concentration of 100 mg/L. It is apparent that the equilibrium concentration in the solution decreases with increasing the amount of adsorbent. This result was anticipated because for a fixed initial solute concentration, increasing the amount of adsorbent provides greater surface area (or adsorption sites).

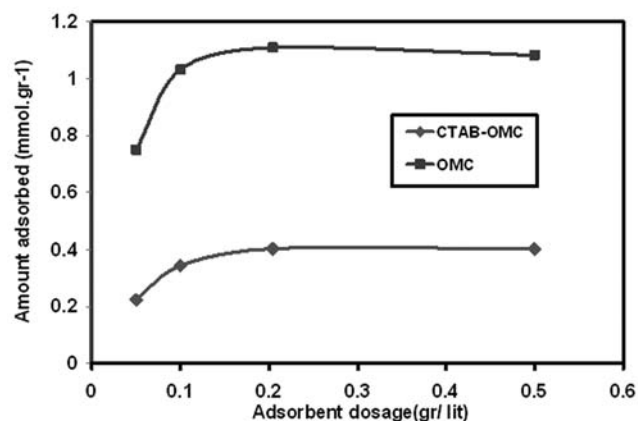


Fig. 5. Effect of CTAB-OMC and OMC amount (0.05–0.5 g/L) on the adsorption of chromate ion ( $\text{pH} = 5$ , initial chromium concentration = 100 ppm, agitation speed = 150 (rpm), temperature = 303 K).

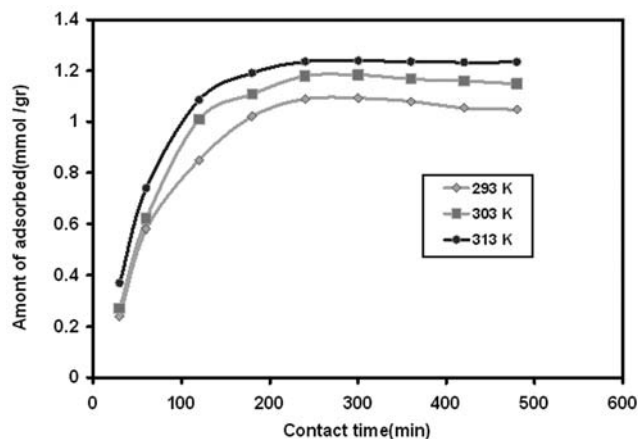


Fig. 6. Effect of temperature of  $\text{Cr(VI)}$  while the initial concentration is 100 mg/L.

### 3.2.2. Effect of temperature

The effect of temperature on the adsorption was studied in the range of 293–313 K for the initial concentration of 100 mg/L of  $\text{Cr(VI)}$ . From the results which are shown in Figure 6, it can be seen that the adsorption capacity of  $\text{Cr(VI)}$  by carbonaceous adsorbents is enhanced with increase in temperature. When the temperature is 313 K, the maximum amount of  $\text{Cr(VI)}$  adsorption reaches 1.2 mmol/g. On the other hand, when the temperature is 293 K, the maximum amount of  $\text{Cr(VI)}$  absorption reaches 1 mmol/g. In the case of physical adsorption, the amount adsorbed increases as the temperature decreases [29], but the amount of  $\text{Cr(VI)}$  onto CTAB-OMC and OMC increases as the temperature increases. This phenomenon may be due to the increase in the rate of intra-particle of  $\text{Cr(VI)}$  into the pores of the adsorbent at higher temperatures which indicates that the diffusion plays an important role in the process of adsorption [30].

### 3.2.3. Effect of pH

The  $\text{Cr(VI)}$  removal from water by an adsorbent is highly depending on the pH of the solution, which subsequently affects the surface charge of the adsorbent, the degree of ionization, and the speciation of the adsorbate species [31]. In aqueous media,  $\text{Cr(VI)}$  anion is not a simple monovalent anion but rather a series of chromate anions depending upon the pH and the solution concentration. Therefore, it was important to study the effect of pH on the removal of  $\text{Cr(VI)}$  onto carbonaceous adsorbents. Figure 7 displays this phenomena, i.e. removal of  $\text{Cr(VI)}$  by CTAB-OMC and OMC, for pH values from 3 to 10. The removal capacities of  $\text{Cr(VI)}$  by CTAB-OMC and OMC were observed to be the highest

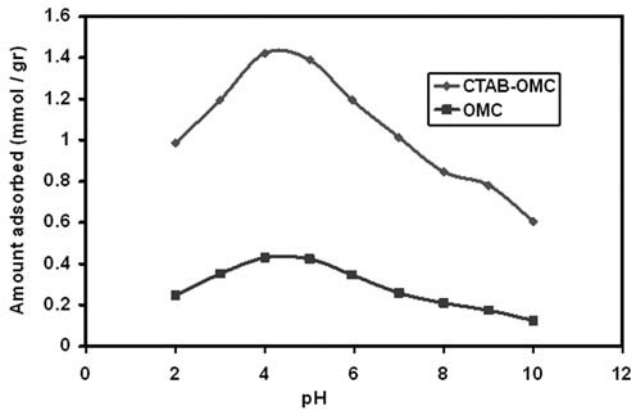
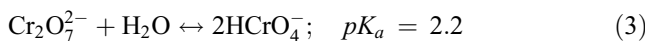
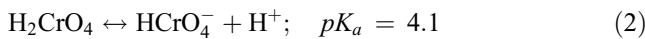
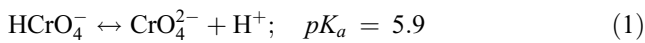


Fig. 7. Effect of pH on chromate ion removal over CTAB-OMC as adsorbent ( $[\text{Cr(VI)}] = 100 \text{ mg/L}$  adsorbent dose =  $0.2 \text{ g/L}$ , agitation speed =  $150 \text{ rpm}$ , temperature =  $303 \text{ K}$ ).

where pH of the solution is 3, and to be the lowest where pH of the solution is 10. The Cr(VI) species may be represented in various forms such as  $\text{H}_2\text{CrO}_4$ ,  $\text{HCrO}_4^-$ ,  $\text{CrO}_4^{2-}$  and  $\text{Cr}_2\text{O}_7^{2-}$  in the solution as a function of pH. The speciation of Cr(VI) is affected by pH of the solution through the following equilibrium [32]:



Above pH 6, the dominant species is the yellow chromate anion,  $\text{CrO}_4^{2-}$ , between pH 2 and 6,  $\text{HCrO}_4^-$  and dichromate ions,  $\text{Cr}_2\text{O}_7^{2-}$  are in equilibrium [33]. From Eq. (1), the major species are  $\text{HCrO}_4^-$  at pH 5 and  $\text{CrO}_4^{2-}$  at pH 7. Because of the distribution of Cr(VI) in the aqueous phase, which is in the form of anions, it is clearly indicated that the OMC which has been modified with cationic surfactant is suitable to adsorb Cr(VI) species at suitable pH values. The adsorption efficiency of Cr(VI) was highest at pH 4 for each of the carbonaceous adsorbents while the adsorption decreased when the pH increased. It is notable that the pH of the solution not only affects the adsorption sites of the sorbent but also the ionic forms of the chromium solutions. On the other hand, the adsorption of Cr(VI) could occur via positively charged ligands. The low pH values lead to an increase in  $\text{H}^+$  ion concentration on the carbon surface which results in strong electrostatic attractions among positively charged AC surfaces and chromium ions when the dominant form of Cr(VI) is  $\text{HCrO}_4^-$ . Therefore, the adsorption of Cr(VI) species is appropriate at low pH values. As the pH increases, the dominant forms of Cr(VI) are  $\text{CrO}_4^{2-}$ ,  $\text{Cr}_2\text{O}_7^{2-}$  while the  $\text{OH}^-$  ions are also increased. The affinity of  $\text{OH}^-$

towards the carbon surfaces is stronger than  $\text{CrO}_4^{2-}$  and  $\text{Cr}_2\text{O}_7^{2-}$  species and thus the adsorption sites are mostly occupied by  $\text{OH}^-$ . As described above, at lower pH values, the Cr(VI) species are present as  $\text{HCrO}_4^-$  and thus require one exchange site for one molecule of Cr(VI) species at that particular pH value. In contrast, at high pH values, the divalent form of Cr(VI) species ( $\text{Cr}_2\text{O}_7^{2-}$ ,  $\text{CrO}_4^{2-}$ ) are dominant and require two exchange sites from the adsorbent for the adsorption to occur. The results have shown higher removal capacities of Cr(VI) species by CTAB-OMC and OMC at lower pH values.

### 3.2.4. Kinetics of adsorption

Any adsorption process is normally controlled by three diffusion steps: (i) transport of the solute from bulk solution to the film surrounding the adsorbent, (ii) from the film to the adsorbent surface, (iii) from the surface to the internal sites followed by binding of the metal ions to the active sites. The slowest step determines the overall rate of the adsorption process and usually it is thought that the step (ii) leads to surface adsorption and the step (iii) leads to intra-particle adsorption [34]. Several kinetic models have been used to explain the mechanism of the adsorption processes. A simple pseudo-first order equation is given by Lagergren equation [34]:

$$\log(q_e - q) = \log q_e - \frac{k_1 t}{2.303} \quad (3)$$

where  $q_e$  and  $q$  are the amounts of Cr (VI) adsorbed (mmol/g) at the equilibrium and time  $t$ , respectively, and  $k_1$  is the rate constant of adsorption ( $\text{min}^{-1}$ ). Plot of  $\log(q_e - q)$  versus  $t$  gives a straight line for first order adsorption kinetics which allows computation of the rate constant  $k_1$ . The calculated  $q_e$ ,  $k_1$  and the corresponding linear regression correlation coefficient values are summarized in Table 2. As it is seen, the calculated linear regression correlation coefficient ( $R^2$ ) is relatively small, 0.988, and the experimental  $q_e$  values did not agree with the calculated values obtained from the linear plots. On the other hand, the pseudo-second order equation based on equilibrium adsorption is expressed as [34]:

$$\frac{t}{q} = \frac{1}{k_2 q_e^2} - \frac{t}{q_e} \quad (4)$$

where  $k_2$  is the pseudo-second order rate constant ( $\text{g/mmol min}$ ),  $q_e$  and  $q$  represent the amount of Cr(VI) adsorbed (mmol/g) at equilibrium and time  $t$ . The equilibrium adsorption capacity ( $q_e$ ), and the second

Table 2  
Pseudo-first order and pseudo-second order constants of Cr(VI) adsorption by CTAB-OMC

Pseudo-first order constants				Pseudo-second order constants			
$q_{e, \text{exp}}$ (mmol/g)	$q_{e, \text{cal}}$ (mmol/g)	$k_1$ (g/mmol min)	$R^2$	$q_{e, \text{exp}}$ (mmol/g)	$q_{e, \text{cal}}$ (mmol/g)	$k_2$ (g/mmol min)	$R^2$
1.45	1.25	0.007	0.988	1.45	1.55	0.008	0.996

order constants ( $k_2$ ) can be determined experimentally from the slope and intercept of plot  $t/q$  versus  $t$ . The calculated  $q_e$ ,  $k_2$  and the corresponding linear regression correlation coefficient values are summarized in Table 2.  $R^2$  value is greater than 0.99. As it is seen from Table 2, the values of  $q_e$  calculated from pseudo-second order kinetics almost agreed with the experimental values of  $q_e$ . These results indicate that the adsorption of Cr(VI) on the prepared activated carbon follows pseudo-second order kinetics. Similar results have been observed for Cr(VI) adsorption with other materials [34,35].

### 3.2.5. Effect of chemical modification

In order to evaluate the efficacy of the prepared adsorbents, the equilibrium adsorption of the chromate ions was studied as a function of equilibrium concentration. The adsorption isotherms of the chromate ions on CTAB-OMC and OMC are shown in Figure 8. It is seen that the order of adsorption in terms of the amount adsorbed (mmol/g) on the carbonaceous adsorbents is: CTAB-OMC > OMC.

Originally, carbon surface have both negative (anionic) and positive (cationic) functional groups to attract free ions from the solutions or suspensions. Apart from wetting and solubilization, surfactants are also capable to produce the electrostatic charge on the surface of the

ordered mesoporous carbon and in turn creating more available active sites for the adsorption. Also, in the presence of cationic surfactants, the presence of CTAB on the surface of ordered mesoporous carbon introduced positive adsorption sites ( $-\text{NH}_2$ ) into the surface of mesoporous carbon. That may be the reason for carbonaceous adsorbents modified by CTAB to increase the removal of chromate ions. Moreover, CTAB-modified mesoporous carbon sorption of chromate ions is rapid, indicating maximum penetration of the adsorbate in less time, due to easy transport of the metal ions into mesopores and micropores.

### 3.2.6. Langmuir and Freundlich isotherms

In order to indicate the sorption behavior and to estimate the adsorption capacity, adsorption isotherms were studied. The adsorption processes of chromate ions onto CTAB-OMC and OMC adsorbents were tested against Langmuir and Freundlich isotherm models. Two commonly used empirical adsorption models, Freundlich and Langmuir, which correspond to heterogeneous and homogeneous adsorbent surfaces, respectively, were employed in this study. The Freundlich model is given by equation (5).

$$\text{Ln}q_e = \text{Ln}K_f + \left(\frac{1}{n}\right) \text{Ln}C_e, \quad (5)$$

where  $k_f$  and  $n$  are the Freundlich constants related to adsorption capacity and intensity, respectively. In the second model, the Langmuir equation assumes maximum adsorption occurs when the surface is covered by the adsorbate, because the number of identical sites on the surface is finite. Equation (6) (Langmuir equation) is given as:

$$\frac{C_e}{q_e} = \left(\frac{1}{q_m b}\right) + \left(\frac{1}{q_m}\right) C_e, \quad (6)$$

where  $q_e$  (mmol  $\text{g}^{-1}$ ) is the amount adsorbed at equilibrium concentration  $C_e$  (mmol  $\text{L}^{-1}$ ),  $q_m$  (mmol  $\text{g}^{-1}$ ) is the Langmuir constant representing maximum monolayer capacity and  $b$  is the Langmuir constant related to the energy of adsorption. The isotherm data has been linearized using the Langmuir equation. The

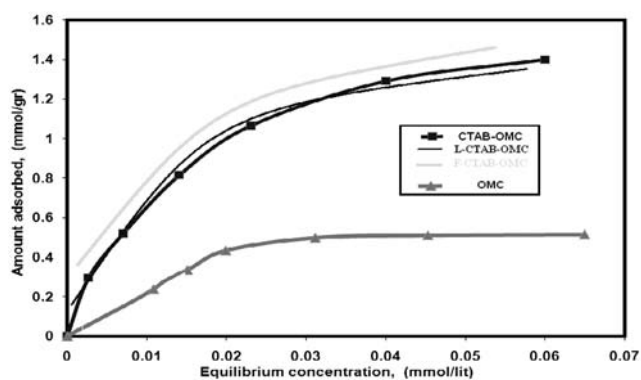


Fig 8. Adsorption isotherm for chromate ion removal on CTAB-OMC and OMC (contact time = 360 min, agitation speed = 150 (rpm), adsorbent dosage = 0.2 g/L, room temperature = 303 K).

Table 3  
Langmuir and Freundlich constants for adsorption of Cr (VI) on CTAB-OMC

Langmuir			Freundlich		
$q_m$ (mmol/g)	$B$ (L/mmol)	$R^2$	$K_F$ (mmol/g)	$n$ (L/mmol)	$R^2$
1.61	89.3	0.996	6.65	1.96	0.979

regression constants are tabulated in Table 3. The high value of correlation coefficient indicates a good agreement between the parameters. The same data is also fitted by the Freundlich equation (Table 3). Moreover, adsorption isotherm of chromate ions onto surfactant-modified adsorbent was fitted with Langmuire and Freundlich isotherms (Figure 8). The values of the correlation coefficients showed that the experimental data conform well to the Langmuir equation.

#### 4. Conclusions

In this work, CTAB, a cationic surfactant was coated on the surface of OMC. The structural order and textural properties of the CTAB-OMC was studied by XRD and nitrogen adsorption. The amount of CTAB on the carbon surface was confirmed by TGA analyses. The surfactant-modified ordered-mesoporous carbon prepared in this work is suitable for the adsorption of aqueous chromate ions from the aqueous solution. Temperature and pH are determinant factors for the Cr(VI) removal. This removal strongly is increased at lower pH values and higher temperatures. Adsorption isotherm was fitted well by Langmuir model.

#### Acknowledgements

Dr. S.N. Ashrafzadeh from IUST is acknowledged for his consultation during the course of this project. Dr. Sh. Garakani from Research Institute of petroleum industry is acknowledged for his assistance in conducting experiments.

#### References

- [1] S.A. Katz and H. Salem, The toxicology of chromium with respect to its chemical speciation: a review, *J. Appl. Toxicol.*, 13 (1993) 217–224.
- [2] M. Costa, Potential hazards of hexavalent chromate in our drinking water, *Toxicol. Appl. Pharmacol.*, 188 (2003) 1–5.
- [3] World Health Organization, Guidelines for Drinking Water Quality vol. 1: recommendation, World Health Organization (WHO), Geneva, 1993.
- [4] S. Rengaraj, C.K. Joo, Y. Kim and J. Yi, Kinetics of removal of chromium from water and electronic process wastewater by ion exchange resins: 1200H, 1500H and IRN97H, *J. Hazard. Mater.*, B102 (2003) 257–275.
- [5] J.W. Patterson, *Industrial Wastewater Treatment Technology*, 2nd ed., Butterworth, Boston, 1985, pp. 217–231.
- [6] I.L. Lagadic, M.K. Mitchell and B.D. Payne, Highly effective adsorption of heavy metal ions by a thiol-functionalized magnesium phyllosilicate clay, *Environ. Sci. Technol.*, 35 (2001) 984–989.
- [7] R. Celis, M.C. Hermosin and J. Cornjo, Heavy metal adsorption by functionalized clays, *Environ. Sci. Technol.*, 34 (2000) 4593–4598.
- [8] N. Zhao, N. Wei, J. Li, Z. Qiao, J. Cui and F. He, Surface properties of chemically modified activated carbons for adsorption rate of Cr(VI), *Chem. Eng. J.*, 115 (2005) 133–138.
- [9] C.A. Basar, A. Karagunduz, B. Keskinler and A. Cakici, Effect of presence of ions on surface characteristics of surfactant modified powdered activated carbon, *Appl. Surf. Sci.*, 218 (2003) 170–175.
- [10] M. Anbia, K. Mohammadi, An Effective Method for the Removal of Dichromate Ion and Furfural from Aqueous Solutions Using a Nanoporous Adsorbent, *Asian J. Chem.* 21, No.5 (2008) 3347–3354.
- [11] M. Anbia, N. Mohammadi, A Nanoporous Adsorbent for the Removal of Furfural from Aqueous Solutions, *Desalination* 249 (2008) 150–153.
- [12] K. Baek, H.H. Lee and J.W. Yang, Micellar-enhanced ultrafiltration for simultaneous removal of ferricyanide and nitrate, *Desalination* 158 (2003) 157–166.
- [13] K. Baek and J.W. Yang, Cross-flow micellar-enhanced ultrafiltration for removal of nitrate and chromate: competitive binding, *J. Hazard. Mater.*, 108 (2004) 119–123.
- [14] K. Baek and J.W. Yang, Simultaneous removal of chlorinated aromatic hydrocarbons, nitrate, and chromate using micellar-enhanced ultrafiltration, *Chemosphere*, 57 (2004) 1091–1097.
- [15] R. Ryoo, S. H. Joo and S. Jun, Synthesis of Highly Ordered Carbon Molecular Sieves via Template-Mediated Structural Transformation, *J. Phys. Chem. B.*, 103 (1999) 7743–7746.
- [16] M. Anbia and S.E. Moradi, Adsorption of naphthalene derived compound from water by chemically oxidized mesoporous carbon. *Chem. Eng. J.*, 148 (2009) 452–458.
- [17] M. Hudson, S.W. Husain and, M. Anbia, Development of new sorbents: I. Ordered porous phase of titanium phosphate, *J. Ir. Chem. Soc.*, 2 (2005) 54–60.
- [18] M. Anbia, M.K. Rofouei and S.W. Husain, Mesoporous lanthanum tungstate as a novel sorbent for removal of heavy metal ions from aqueous media, *Asian J. Chem.*, 19 (2007) 3862–3868.
- [19] M. Anbia, M.K. Rofouei and S.W. Husain, Development of new adsorbents: II. sorption of toxic metals on mesoporous lanthanum silicate, *Oriental. J. Chem.*, 21 (2005) 199–206.
- [20] M. Anbia, M.K. Rofouei and S.W. Husain, Synthesis of mesoporous lanthanum phosphate and its use as a novel sorbent, *Chin. J. Chem.*, 24 (2006) 1026–1030.
- [21] M. Anbia and S.E. Moradi, Removal of naphthalene from petrochemical wastewater streams using carbon nanoporous adsorbent, *Appl. Surf. Sci.*, 255 (2009) 5041–5047.
- [22] Y.R. Lin and H. Teng, Mesoporous carbons from waste tire char and their application in wastewater discoloration, *Micropor. Mesopor. Mater.*, 54 (2002) 167–173.
- [23] M. Gun'ko, W.R. Betz, S. Patel, M.C. Murphy and S.V. Mikhalovsky, Adsorption of lipopolysaccharide on carbon sieves, *Carbon*, 44 (2006) 1258–1264.
- [24] Y. Shao, L. Wang, J. Zhang and M. Anpo, Synthesis of hydrothermally stable and long-range ordered Ce-MCM-48 and Fe-MCM-48 materials, *Micropor. Mesopor. Mater.*, 109 (2005) 20835–20841.



- [25] M. Ghiaci, R. Kia, A. Abbaspur and F. Seyedejn-Azad, Adsorption of chromate by surfactant-modified zeolites and MCM-41 molecular sieve, *Sep. Purif. Technol.* 40 (2004) 285–295.
- [26] R. Crisafulli, M.A. Milhome, R.M. Cavalcante, E.R. Silveira, D. Keukeleire and R.F. Nascimento, Removal of some polycyclic aromatic hydrocarbons from petrochemical wastewater using low-cost adsorbents of natural origin, *Bioresour. Technol.*, 99 (2008) 4515–4519.
- [27] Y. Xun, Z. Shu-Ping, X. Wei, C. Hong-You, D. Xiao-Dong, L. Xin-Mei and Y. Zi-Feng, Aqueous dye adsorption on ordered mesoporous carbons, *J. Coll. Interf. Sci.*, 310 (2007) 83–87.
- [28] S. Jun, S.H. Joo, R. Ryoo, M. Kruk, M. Jaroniec, Z. Liu, T. Ohsuna and O. Terasaki, Synthesis of new nanoporous carbon with hexagonally ordered mesostructure, *J. Am. Chem. Soc.*, 122 (2000) 10712–10718.
- [29] N. Kawasaki, R. Bun-ei, F. Ogata, S. Tanei and S. Tanada, Water treatment technology using carbonaceous materials produced from vegetable biomass, *J. Water Environ. Technol.*, 4 (2006) 73–82.
- [30] C. Namasivayam and R.T. Yamuna, Adsorption of chromium (VI) by a low-cost adsorbent: biogas residual slurry, *Chemosphere*, 30 (1995) 561–578.
- [31] R. Schumi, H.M. Krieg and K. Keizer, Adsorption of Cu(II) and Cr(VI) ions by chitosan: kinetics and equilibrium, *Water SA*, 27 (2001) 1–7.
- [32] F.A. Cotton and G. Wilkinson, *Advanced Inorganic Chemistry*, 5th ed., Wiley, New York, 1998.
- [33] Z. Li, Influence of solution pH and ionic strength on chromate uptake by surfactant-modified zeolite, *J. Environ. Eng.*, 130 (2004) 205–208.
- [34] A. Sharma and K.G. Bhattacharyya, Adsorption of chromium(VI) on *Azadirachta Indica* (Neem) leaf powder, *Adsorption*, 10 (2004) 327–338.
- [35] N.K. Hamadi, X.D. Chen, M.M. Farid and M.G.Q. Lu, Adsorption kinetics for the removal of chromium(VI) from aqueous solution by adsorbents derived from used tyres and sawdust, *Chem. Eng. J.*, 84 (2001) 95–105.